



ACADEMIC  
PRESS

Available online at [www.sciencedirect.com](http://www.sciencedirect.com)

SCIENCE @ DIRECT®

Journal of Magnetic Resonance 160 (2003) 52–58

JMR

Journal of  
Magnetic Resonance

[www.elsevier.com/locate/jmr](http://www.elsevier.com/locate/jmr)

## Multiplex phase cycling

Natala Ivchenko,<sup>a</sup> Colan E. Hughes,<sup>b,1</sup> and Malcolm H. Levitt<sup>a,\*</sup>

<sup>a</sup> Department of Chemistry, Southampton University, Highfield, Southampton SO17 1BJ, UK

<sup>b</sup> Physical Chemistry Division, Stockholm University, S-10691 Sweden

Received 15 July 2002; revised 25 October 2002

### Abstract

We discuss a new class of phase cycling procedures, in which a set of individual phase-shifted transients are stored separately in the computer and processed afterwards to yield the separated NMR signals from two or more coherence transfer pathways. In the case of two-dimensional double-quantum spectroscopy, this multiplex acquisition procedure allows the acquisition of pure-absorption spectra in only 62.5% of the time needed by previous methods.

© 2002 Elsevier Science (USA). All rights reserved.

**Keywords:** Phase cycling; Coherence transfer pathways; Multiplex phase cycles; Pure-absorption phase

### 1. Introduction

In many cases, the timespan of an NMR experiment is determined by the need to complete the phase cycle, rather than the necessity of obtaining a sufficiently large signal-to-noise ratio. There is much interest in shorter phase cycles, such as the cogwheel cycles introduced recently by this group [1], or the abbreviated phase cycles studied by McClung and co-workers [2].

In some cases, the variation of the radio-frequency phases in a set of acquired transients is used for multiple purposes. Consider, for example, the acquisition of pure-absorption 2D spectra by the States–Ruben–Haberkorn (SRH) scheme [3]. In this popular method, phase shifts are used (i) to eliminate interference from undesirable NMR signals or receiver artefacts, and (ii) to provide a set of cosine and sine-modulated signals, from which pure-absorption 2D spectra may be constructed, while retaining information on the sense of the precession frequency during the evolution interval  $t_1$ . For example, in pure-absorption 2Q spectroscopy, eight acquired transients are required in the SRH method for

every  $t_1$  increment: four transients for acquisition of a cosine-modulated data set, with suppression of signals from coherences which do not have order  $\pm 2$  during  $t_1$ ; and four transients for acquisition of a sine-modulated data set, with similar selection properties.

In this article, we show that these two tasks may be compressed into one, providing a saving in experimental time. This gain comes at the modest cost of increased data storage space and somewhat more complicated post-processing of the data. In the new method, only *five* transients are acquired for every  $t_1$  increment and stored *separately* in the computer. The set of five independent transients is processed in two different ways to obtain separate signals for the (+2)-quantum and the (–2)-quantum pathways. The pure-absorption 2D spectrum, with discrimination of the signs of the precession frequency, is then constructed from these two independent data sets.

This is just one example of a general class of phase cycles, which we call *multiplex* phase cycles. In a multiplex phase cycle, the different transients acquired in a phase cycling scheme are not immediately combined in the data acquisition device. Instead, the acquired transients are stored individually in the computer memory and processed afterwards to obtain independent signals from two or more distinct sets of coherence transfer pathways. This procedure allows the experimental time to be used more efficiently and ensures that useful

\* Corresponding author. Fax: +44-23-8059-3781.

E-mail address: [Malcolm.Levitt@soton.ac.uk](mailto:Malcolm.Levitt@soton.ac.uk) (M.H. Levitt).

<sup>1</sup> Current address: Department for NMR-Based Structural Biology, Max Planck Institute for Biophysical Chemistry, 37077 Göttingen, Germany.

signals are not already discarded at the stage of signal averaging.

### 2. Conventional phase cycling

Phase cycling involves the linear superposition of NMR signals acquired with different spectrometer phase settings. These include the radio-frequency phases of the different pulse sequence blocks, denoted here  $\phi_A, \phi_B, \phi_C, \dots$ , the radio-frequency phase of the reference signal during acquisition of the quadrature NMR signal, denoted  $\phi_{\text{rec}}$ , and the post-digitization phase shift applied at the output of the analog-to-digital converters (ADCs), denoted  $\phi_{\text{dig}}$  [4]. In general, these phases follow a cyclic scheme of length  $N$ , so that each of these phases is specified by a counter denoted  $m$ , where  $m = 0, 1, \dots, N - 1$ . In conventional data acquisition, the quadrature NMR signals are summed in the signal accumulation device according to

$$s(t) = \sum_{m=0}^{N-1} s_m(t). \quad (1)$$

The selection of NMR signals under phase cycling is conveniently specified in terms of the coherence transfer pathway (CTP), defined as the history of coherence orders leading to a particular signal contribution [5–7]. A general coherence transfer pathway has the form  $\mathbf{p} = \{0, p_{AB}, p_{BC}, \dots, -1\}$ , where  $p_{AB}$  is the coherence order between blocks  $A$  and  $B$ ,  $p_{BC}$  is the coherence order between blocks  $B$  and  $C$ , and so on. The pathway starts with order 0 to indicate a reproducible initial state of spin populations and ends with order  $-1$  to indicate detection of the quadrature NMR signal [5–7]. The notation for the block phases and pathway orders is summarized in Fig. 1.

In conventional phase cycling, the spectrometer phases are selected so that the following equation is satisfied:

$$N^{-1} \sum_{m=0}^{N-1} \exp\{-i\Phi_{\mathbf{p}}(m)\} = \begin{cases} 1 & \text{if } \mathbf{p} \in \mathcal{P}, \\ 0 & \text{otherwise,} \end{cases}$$

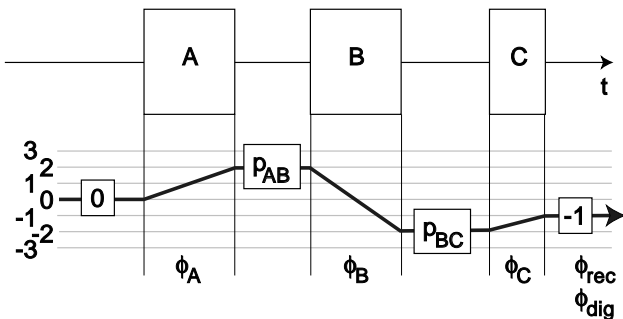


Fig. 1. A pulse sequence consisting of three blocks,  $A$ ,  $B$ , and  $C$ , and a coherence transfer pathway  $\{0, p_{AB}, p_{BC}, -1\}$ . In the example shown, the coherence order between blocks  $A$  and  $B$  is  $p_{AB} = +2$ , while the coherence order between blocks  $B$  and  $C$  is  $p_{BC} = -2$ .

where  $\mathcal{P} = \{\mathbf{p}_0, \mathbf{p}_1, \dots\}$  represents a set of one or more “desired” coherence transfer pathways. The overall pathway phase  $\Phi_{\mathbf{p}}$  is defined by

$$\Phi_{\mathbf{p}}(m) = \phi_A \Delta p_A(m) + \phi_B \Delta p_B(m) + \dots + \phi_{\text{rec}}(m) + \phi_{\text{dig}}(m), \quad (2)$$

where  $\{\Delta p_A, \Delta p_B, \dots\}$  indicates the changes in coherence order induced by the pulse sequence blocks  $\{A, B, \dots\}$ . The construction rules for phase cycles which select signals from one or more desired coherence transfer pathways  $\mathcal{P} = \{\mathbf{p}_0, \mathbf{p}_1, \dots\}$ , suppressing all others, are well established [5–7]. In some cases, the recently developed “cogwheel” phase cycles [1] accomplish this task in a particularly small number of steps  $N$ .

### 3. Multiplex phase cycling

In multiplex phase cycling, the individual quadrature signal transients  $s_m(t)$  are stored individually in the computer. The set of  $N$  acquired transients is processed according to the equation

$$s^{(M)}(t) = \sum_{m=0}^{N-1} s_m(t) \exp\{-i\phi_{\text{num}}^{(M)}(m)\}, \quad (3)$$

where  $\phi_{\text{num}}^{(M)}(m)$  is a numerical phase shift, readily implemented by complex multiplication in the computer. In general, the same set of  $N$  transients is subjected to several different sets of numerical phase shifts, leading to a set of post-processed signals  $s^{(M)}(t)$ , where the index  $M$  distinguishes the different post-processing modes. If the set of numerical phase shifts  $\{\phi_{\text{num}}^{(M)}(0), \phi_{\text{num}}^{(M)}(1), \dots, \phi_{\text{num}}^{(M)}(N - 1)\}$  is used, then the selected signals belong to one set of coherence transfer pathways  $\mathcal{P}^{(M)} = \{\mathbf{p}_0^{(M)}, \mathbf{p}_1^{(M)}, \dots\}$ , while if a different set of numerical phase shifts  $\{\phi_{\text{num}}^{(M')}(0), \phi_{\text{num}}^{(M')}(1), \dots, \phi_{\text{num}}^{(M')}(N - 1)\}$  is used, then the selected signals belong to a different set of coherence transfer pathways  $\mathcal{P}^{(M')} = \{\mathbf{p}_0^{(M')}, \mathbf{p}_1^{(M')}, \dots\}$ , and so on.

This property may be arranged by choosing the spectrometer phases  $\{\phi_A, \phi_B, \phi_C, \dots, \phi_{\text{rec}}, \phi_{\text{dig}}\}$  and the sets of numerical phase shifts  $\{\phi_{\text{num}}^{(M)}, \phi_{\text{num}}^{(M')}, \dots\}$ , such that the following equations are satisfied:

$$N^{-1} \sum_{m=0}^{N-1} \exp\left\{-i\left[\Phi_{\mathbf{p}}(m) + \phi_{\text{num}}^{(M)}(m)\right]\right\} = \begin{cases} 1 & \text{if } \mathbf{p} \in \mathcal{P}^{(M)}, \\ 0 & \text{otherwise,} \end{cases}$$

$$N^{-1} \sum_{m=0}^{N-1} \exp\left\{-i\left[\Phi_{\mathbf{p}}(m) + \phi_{\text{num}}^{(M')}(m)\right]\right\} = \begin{cases} 1 & \text{if } \mathbf{p} \in \mathcal{P}^{(M')}, \\ 0 & \text{otherwise.} \end{cases}$$

⋮

(4)

Multiplex phase cycling allows the filtering out of signals from the pathway set  $\mathcal{P}^{(M)}$ , or from the pathway set  $\mathcal{P}^{(M')}$ , and so on, using the *same* acquired experimental data. In some cases, this can lead to significant time savings.

The multiplex principle was mentioned in passing by Bodenhausen et al. [6], but the potential advantages were not worked through. In this communication, we show that the multiplex principle reduces the time required to acquire pure-absorption double-quantum 2D spectra.

#### 4. Pure-absorption double-quantum spectroscopy

A 2D double-quantum experiment consists of two pulse sequence blocks: an excitation block *A*, which generates double-quantum coherence, a variable evolution interval  $t_1$ , a reconversion block *B*, which converts the double-quantum coherences into observable  $(-1)$ -quantum coherences, and a detection interval  $t_2$  during which the quadrature NMR signal is acquired. The interesting NMR signals come from the two double-quantum pathways  $\mathbf{p}^{(+2)} = \{0, +2, -1\}$  and  $\mathbf{p}^{(-2)} = \{0, -2, -1\}$ . Double-quantum phase-cycling procedures select signals from one or both of these two pathways, while suppressing other signals, such as those from the single-quantum pathways  $\mathbf{p}^{(\pm 1)} = \{0, \pm 1, -1\}$  and the zero-quantum pathway  $\mathbf{p}^{(0)} = \{0, 0, -1\}$ . In this paper, we ignore higher-quantum pathways such as  $\mathbf{p}^{(\pm 3)} = \{0, \pm 3, -1\}$  and  $\mathbf{p}^{(\pm 4)} = \{0, \pm 4, -1\}$ , which normally are only weakly excited in systems of spins 1/2.

An example pulse sequence is shown in Fig. 2a. This sequence is used for magic-angle spinning (MAS) NMR of coupled  $^{13}\text{C}$  spins in organic solids, and employs the C7 double-quantum recoupling method [8].

Both pathways  $\mathbf{p}^{(\pm 2)}$  are needed to obtain pure-absorption 2D spectra. In the usual procedure, this is taken into account by using a phase cycle for which the set of “desired” signal pathways is given by  $\mathcal{P} = \{\mathbf{p}^{(+2)}, \mathbf{p}^{(-2)}\}$ . Since the orders  $(\pm 2)$  are separated by four units, this requires a 4-step phase cycle ( $N = 4$ ), one example being

$$\begin{aligned}\phi_A(m) &= m\pi/2, \\ \phi_B(m) &= \phi_{\text{rec}}(m) = 0, \\ \phi_{\text{dig}}(m) &= m\pi.\end{aligned}\quad (5)$$

This phase cycle suppresses signals from the zero and single-quantum pathways  $\mathbf{p}^{(0)}$  and  $\mathbf{p}^{(\pm 1)}$ , as well as the higher-quantum pathways such as  $\mathbf{p}^{(\pm 3)}$ ,  $\mathbf{p}^{(\pm 4)}$ , and so on. The effect of four-step phase cycling is illustrated by the pathway diagram in Fig. 2b.

However, since this phase cycle passes signals from *both* of the double-quantum pathways  $\mathbf{p}^{(+2)}$  and  $\mathbf{p}^{(-2)}$ , it is not immediately possible to determine the sign of the double-quantum precession frequency in the  $t_1$  interval. There are a number of ways round this problem, but all require doubling the number of acquired transients. For example, in the SRH method [3], a second set of ex-

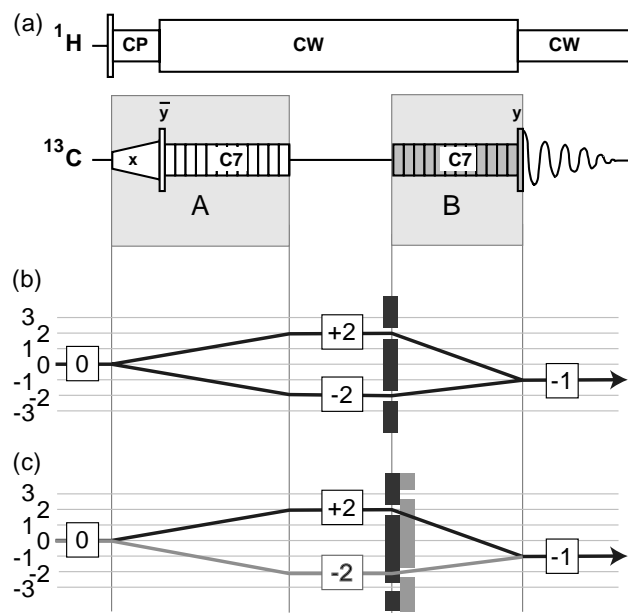


Fig. 2. (a) Pulse sequence for double-quantum  $^{13}\text{C}$  spectroscopy of organic solids. The blocks *A* and *B* are referenced in the text. (b) Coherence transfer pathway diagram for conventional 4-step phase cycling. Both  $(\pm 2)$ -quantum coherences are selected, allowing construction of a pure-absorption 2D double-quantum spectrum by the SRH or TPPI procedures. Note that the barrier has holes separated by four units. (c) Coherence transfer pathway diagram for 5-step phase cycling. Normally, either the  $(+2)$ -quantum or the  $(-2)$ -quantum pathways must be selected, but multiplexing allows both pathways to be constructed from the same data set. There are two alternative barriers, each with holes separated by five units.

periments is performed, in which the double-quantum phase is shifted by  $\pi/2$ . This may be done by shifting the overall phase of block *A* by  $\pi/4$ . The two data sets are combined after data acquisition to produce pure-absorption 2D double-quantum spectra.

A second popular method involves shifting the effective frequency of the double-quantum evolution by incrementing the phase of block *A* in synchrony with the evolution interval  $t_1$ . This is called time-proportional phase incrementation (TPPI) [7,9,10]. By shifting the double-quantum frequencies so that all of the  $(-2)$ -quantum frequencies are positive and all of the  $(+2)$ -quantum frequencies are negative, it is possible to separate these signals completely. However, this method requires a doubling of the spectral bandwidth in the indirectly acquired dimension and hence a doubling of the number of acquired  $t_1$  increments, if the same spectral resolution is to be achieved. Hence, the TPPI method requires the same overall number of transients as the SRH method.

In the multiplex approach, one recognizes instead that although signals from both  $\mathbf{p}^{(\pm 2)}$  pathways are desirable, they must also be *separated* if the sign of the double-quantum precession is to be determined. We therefore require the construction of two different 2D

NMR signals from the same set of acquired transients, according to Eq. (3), i.e.,

$$s^{(\pm 2)}(t_1, t_2) = \sum_{m=0}^{N-1} s_m(t_1, t_2) \exp\{-i\phi_{\text{num}}^{(\pm 2)}(m)\}, \quad (6)$$

where  $s^{(+2)}$  consists only of signals from the pathway  $\mathbf{p}^{(+2)} = \{0, +2, -1\}$  and  $s^{(-2)}$  consists only of signals from the pathway  $\mathbf{p}^{(-2)} = \{0, -2, -1\}$ . This is arranged by choosing the phases so as to satisfy the multiplex selection rules Eq. (4), which in this case correspond to

$$N^{-1} \sum_{m=0}^{N-1} \exp\left\{-i\left[\Phi_p(m) + \phi_{\text{num}}^{(+2)}(m)\right]\right\} = \begin{cases} 1 & \text{if } \mathbf{p} = \mathbf{p}^{(+2)}, \\ 0 & \text{otherwise,} \end{cases}$$

$$N^{-1} \sum_{m=0}^{N-1} \exp\left\{-i\left[\Phi_p(m) + \phi_{\text{num}}^{(-2)}(m)\right]\right\} = \begin{cases} 1 & \text{if } \mathbf{p} = \mathbf{p}^{(-2)}, \\ 0 & \text{otherwise.} \end{cases} \quad (7)$$

The first part of Eq. (7) is readily satisfied using standard construction procedures [5–7]. At least five phase cycle steps are required to select the signal pathway  $\mathbf{p}^{(+2)}$  while suppressing the four neighbouring signal pathways  $\{\mathbf{p}^{(+1)}, \mathbf{p}^{(0)}, \mathbf{p}^{(-1)}, \mathbf{p}^{(-2)}\}$ . One solution with  $N = 5$  is as follows:

$$\begin{aligned} \phi_A(m) &= 2\pi m/5, \\ \phi_B(m) &= \phi_{\text{rec}}(m) = 0, \\ \phi_{\text{dig}}(m) + \phi_{\text{num}}^{(+2)}(m) &= -4\pi m/5. \end{aligned} \quad (8)$$

The last line follows from the order changes  $\Delta p_A = +2$  and  $\Delta p_B = -3$  for the pathway  $\mathbf{p}^{(+2)} = \{0, +2, -1\}$ .

Similarly, the signal pathway  $\mathbf{p}^{(-2)}$  may be selected while suppressing the four neighbouring signal pathways  $\{\mathbf{p}^{(+2)}, \mathbf{p}^{(+1)}, \mathbf{p}^{(0)}, \mathbf{p}^{(-1)}\}$  by using the following phases:

$$\begin{aligned} \phi_A(m) &= 2\pi m/5, \\ \phi_B(m) &= \phi_{\text{rec}}(m) = 0, \\ \phi_{\text{dig}}(m) + \phi_{\text{num}}^{(-2)}(m) &= +4\pi m/5. \end{aligned} \quad (9)$$

The last line follows from the order changes  $\Delta p_A = -2$  and  $\Delta p_B = +1$  for the pathway  $\mathbf{p}^{(-2)} = \{0, -2, -1\}$ .

Since the radio-frequency phases in Eqs. (8) and (9) are identical, multiplex phase cycling is feasible. One solution uses the following spectrometer phases:

$$\begin{aligned} \phi_A(m) &= 2\pi m/5, \\ \phi_B(m) &= \phi_{\text{rec}}(m) = \phi_{\text{dig}}(m) = 0 \end{aligned} \quad (10)$$

and the following numerical phase shifts:

$$\phi_{\text{num}}^{(\pm 2)}(m) = \mp 4\pi m/5. \quad (11)$$

For each  $t_1$  increment, the set of 5 stored transients obtained with the spectrometer phases in Eq. (10) is post-processed in the computer according to the procedure in Eq. (6), which in this case corresponds to

$$\begin{aligned} s^{(+2)}(t_1, t_2) &= \sum_{m=0}^4 s_m(t_1, t_2) \exp\{i4\pi m/5\}, \\ s^{(-2)}(t_1, t_2) &= \sum_{m=0}^4 s_m(t_1, t_2) \exp\{-i4\pi m/5\}. \end{aligned} \quad (12)$$

The result is two 2D signal surfaces  $s^{(\pm 2)}(t_1, t_2)$ , each containing one of the separated  $(\pm 2)$ -quantum signals.

Note that this separation is achieved without acquiring a second set of data. It is therefore possible to reduce the number of acquired transients per  $t_1$  increment from 8 to 5. The only disadvantages of multiplex phase cycling are (i) the more complicated data storage and processing and (ii) the non-suppression of triple-quantum signals. In the most cases, the triple-quantum signals are expected to be very weak (if necessary, they may be suppressed by using 6 steps instead of 5).

The effect of multiplex phase cycling is depicted in Fig. 2c, which shows two alternative coherence selection strategies, each represented by a barrier containing holes separated by five units, but with a relative shift of 1 unit.

The separated  $(\pm 2)$ -quantum signals obtained by Eq. (12) may be fed into the SRH procedure. Providing that the usual conditions are satisfied (real and identical amplitudes for the  $(\pm 2)$ -quantum pathways [4,7]), this leads to pure-absorption 2Q spectra, with discrimination of the sign of the double-quantum precession.

Explicitly, the cosine and sine-modulated 2D signals are constructed using

$$\begin{aligned} s^{\cos}(t_1, t_2) &= \frac{1}{2} \{s^{(+2)}(t_1, t_2) + s^{(-2)}(t_1, t_2)\}, \\ s^{\sin}(t_1, t_2) &= \frac{1}{2i} \{s^{(+2)}(t_1, t_2) - s^{(-2)}(t_1, t_2)\}. \end{aligned} \quad (13)$$

Each signal set is subjected to a Fourier transform in the  $t_2$  dimension, according to

$$\begin{aligned} S^{\cos}(t_1, \omega_2) &= \int_0^{\infty} dt_2 s^{\cos}(t_1, t_2) \exp\{-i\omega_2 t_2\}, \\ S^{\sin}(t_1, \omega_2) &= \int_0^{\infty} dt_2 s^{\sin}(t_1, t_2) \exp\{-i\omega_2 t_2\}. \end{aligned} \quad (14)$$

A new 2D signal is constructed from the real parts of the Fourier transforms, according to

$$s^{\text{SRH}}(t_1, \omega_2) = \text{Re}\{S^{\cos}(t_1, \omega_2)\} + i\text{Re}\{S^{\sin}(t_1, \omega_2)\}. \quad (15)$$

Fourier transformation of this signal with respect to  $t_1$  leads to the pure-absorption 2D spectrum:

$$S^{\text{SRH}}(\omega_1, \omega_2) = \int_0^{\infty} dt_1 s^{\text{SRH}}(t_1, \omega_2) \exp\{-i\omega_1 t_1\}. \quad (16)$$

It is also possible to generate the sine and cosine-modulated signals from the five acquired transients directly, according to

$$s^{\cos}(t_1, t_2) = \sum_{m=0}^4 s_m(t_1, t_2) \cos\{4\pi m/5\},$$

$$s^{\sin}(t_1, t_2) = \sum_{m=0}^4 s_m(t_1, t_2) \sin\{4\pi m/5\}. \quad (17)$$

The cosine and sine-modulated signals are then processed according to Eqs. (14)–(16). This is numerically more efficient.

There are numerous other ways of implementing the multiplex procedure for pure-absorption double-quantum spectroscopy. For example, the reconversion block may be cycled instead of the excitation block, leading to

$$\phi_A(m) = \phi_{\text{rec}}(m) = \phi_{\text{dig}}(m) = 0,$$

$$\phi_B(m) = 2\pi m/5. \quad (18)$$

The five acquired transients are processed according to Eq. (6), using the numerical phase shifts given below:

$$\phi_{\text{num}}^{(-2)}(m) = -2\pi m/5,$$

$$\phi_{\text{num}}^{(+2)}(m) = +6\pi m/5. \quad (19)$$

The cosine and sine-modulated data sets  $s^{\cos}(t_1, t_2)$  and  $s^{\sin}(t_1, t_2)$  are extracted from  $s^{(\pm 2)}(t_1, t_2)$  by applying Eq. (13). The pure-absorption 2D spectrum is constructed by the following the SRH procedure [Eqs. (14)–(16)].

Post-processing of two or more independent data sets has been used before to generate pure-absorption 2D data. Consider, for example, the early explorations of the Ernst and Freeman groups [11,12] and the pure-absorption MAS-exchange acquisition schemes of Hagemeyer et al. [13]. However, all of these techniques use substantial timing changes or other variations of the RF pulse sequences to generate the independent data sets, while the multiplex, SRH and TPPI methods only use variations of the RF phases.

## 5. Results

Fig. 3 shows 2D double-quantum  $^{13}\text{C}$  spectra of polycrystalline  $[\text{U}]^{13}\text{C}$ -L-alanine, obtained at a magic-angle spinning frequency of 9.500 kHz in a field of 4.7 T. Longitudinal  $^{13}\text{C}$  magnetization was generated by ramped cross-polarization from the protons [14], followed by a strong  $\pi/2$  pulse, shifted in phase with respect to the cross-polarization field by  $\pi/2$ . Double-quantum coherences were generated by a C7 pulse sequence [8] of duration  $\tau_{\text{exc}} = 451.2 \mu\text{s}$ . The  $(\pm 2)$ -quantum coherences were allowed to evolve in the presence of strong proton decoupling for the  $t_1$  interval. A second C7 pulse sequence of duration  $210.6 \mu\text{s}$  re-generated longitudinal  $^{13}\text{C}$  magnetization, which was converted into observable  $(-1)$ -quantum coherences by a final  $\pi/2$  pulse.

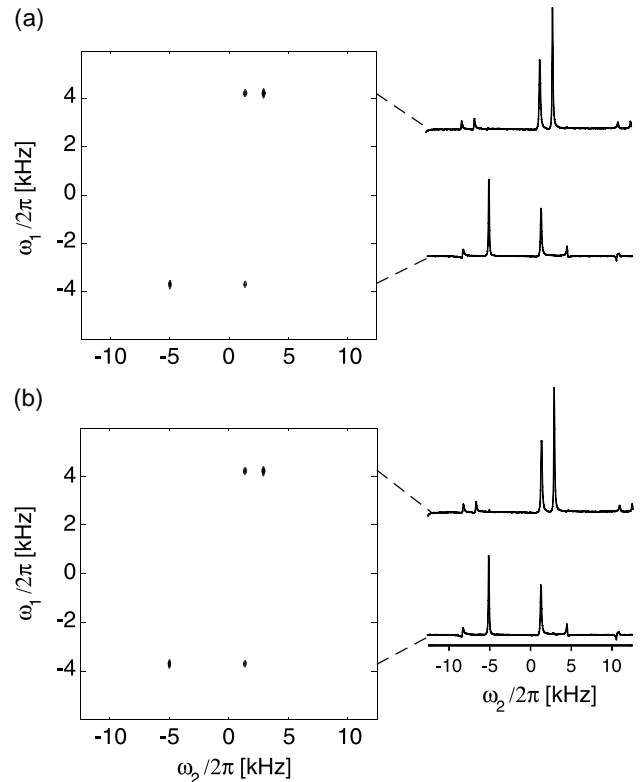


Fig. 3. Experimental pure-absorption double-quantum  $^{13}\text{C}$  spectrum of polycrystalline  $[\text{U}]^{13}\text{C}$ -L-alanine, in a magnetic field of 4.7 T. The spinning frequency was 9.500 kHz. The spectra were obtained on a Varian Chemagnetics Infinity-200 Spectrometer using a 4 mm zirconia rotor. A C7 sequence of duration  $451.2 \mu\text{s}$  was used to excite the  $(\pm 2)$ -quantum coherences. The double-quantum coherences were converted into observable transverse magnetization by a C7 sequence of duration  $210.6 \mu\text{s}$ , followed by a strong  $\pi/2$  pulse. In both cases, the signal surface was compiled using 128 increments of the  $t_1$  evolution interval, in steps of  $83.3 \mu\text{s}$ . The single-quantum axis is horizontal; the double-quantum axis is vertical. (a) Spectrum obtained with the SRH method. The cosine and sine-modulated signal surfaces were both acquired by summing 20 transients per  $t_1$  increment, using the 4-step phase cycles specified in Eq. (20) and Eq. (21). (b) Spectrum obtained with the 5-step multiplex phase cycle specified in Eq. (18). Each of the five data sets was acquired with eight transients per  $t_1$  increment, and processed using the numerical phase shifts specified in Eq. (19). Both spectra show the typical double-quantum pattern of a 3-spin-1/2 system. The signal-to-noise ratios are comparable, as expected from the fact that both spectra were acquired with 40 transients in total per  $t_1$  increment.

The  $^{13}\text{C}$  RF fields during the cross-polarization interval, the strong  $\pi/2$  pulses, and the C7 sequences, corresponded to nutation frequencies of 53.0, 69.5, and 66.5 kHz, respectively. The  $^1\text{H}$  RF fields during the cross-polarization interval, the C7 sequences, and the signal acquisition interval corresponded to nutation frequencies of 48, 99, and 91 kHz, respectively.

Fig. 3a shows a 2D spectrum obtained with the SRH method. In order to acquire the cosine-modulated data set  $s^{\cos}(t_1, t_2)$ , the evolution interval  $t_1$  was incremented in 128 steps of  $83.3 \mu\text{s}$ . Twenty transients were acquired

for each  $t_1$  increment, with the RF phases on the  $^{13}\text{C}$  channel following a standard 4-step phase cycle:

$$\begin{aligned}\phi_A^{\text{cos}}(m) &= 0, \\ \phi_B^{\text{cos}}(m) &= \pi m/2, \\ \phi_{\text{rec}}^{\text{cos}}(m) &= 0, \\ \phi_{\text{dig}}^{\text{cos}}(m) &= -\pi m/2.\end{aligned}\quad (20)$$

A sine-modulated data set  $s^{\text{sin}}(t_1, t_2)$  was acquired with the same number of  $t_1$  increments and transients, using the modified phases:

$$\begin{aligned}\phi_B^{\text{sin}}(m) &= -\pi/4, \\ \phi_B^{\text{sin}}(m) &= \pi m/2, \\ \phi_{\text{rec}}^{\text{sin}}(m) &= 0, \\ \phi_{\text{dig}}^{\text{sin}}(m) &= -\pi m/2.\end{aligned}\quad (21)$$

In both cases, the “excitation block”  $A$  refers to the  $^{13}\text{C}$  cross-polarization field (phase  $\phi_1$ ), the first  $\pi/2$  pulse (phase  $\phi_2$ ), and the first C7 sequence (overall phase  $\phi_3$ ). The phases of these RF elements are given in terms of the block phase  $\phi_A$  by:

$$\begin{aligned}\phi_1 &= \phi_A, \\ \phi_2 &= \phi_A - \pi/2, \\ \phi_3 &= \phi_A.\end{aligned}\quad (22)$$

The “reconversion” block  $B$  refers to the second C7 sequence (phase  $\phi_4$ ) and the last strong  $\pi/2$  pulse (phase  $\phi_5$ ). The overall RF phases of these elements are given in terms of the block phase  $\phi_B$  by:

$$\phi_4 = \phi_5 = \phi_B + \pi/2 + \omega_r t_1, \quad (23)$$

where  $\omega_r$  is the angular spinning frequency and  $t_1$  is the variable evolution interval between the two blocks. The dependence of the C7 reconversion phase on the evolution interval takes into account the rotation of the sample between the two C7 pulse sequences [15].

The two data sets  $s^{\text{cos}}(t_1, t_2)$  and  $s^{\text{sin}}(t_1, t_2)$  were subjected to SRH data processing [Eqs. (14)–(16)] to obtain the two dimensional spectrum  $S^{\text{SRH}}(\omega_1, \omega_2)$ , the real part of which is shown in Fig. 3a. The spectrum displays strong peaks from the two double-quantum coherences involving directly-bonded  $^{13}\text{C}$  spin pairs in the three-spin system. As expected, the peaks are approximately in pure-absorption phase. The small phase deviations may be attributed to imperfect performance of the C7 sequences.

The spectrum shown in Fig. 3b was obtained using the same number of  $t_1$  increments and the same increment in  $t_1$ , but with the set of spectrometer phases specified in Eq. (18). In this case, eight transients were acquired for each of the five phase cycle steps, so that 40

transients in total were acquired per  $t_1$  increment, allowing a direct comparison of the signal-to-noise ratio with Fig. 3a. The five data sets were stored separately and processed using the numerical phase shifts in Eq. (19) to obtain the  $(\pm 2)$ -quantum signal surfaces  $s^{(\pm 2)}(t_1, t_2)$ . These data matrices were combined according to Eq. (13) in order to obtain the cosine and sine-modulated signal surfaces, which were processed using the SRH procedure as before. The real part of the resulting spectrum is shown in Fig. 3b. It is almost identical to that shown in Fig. 3a and has an indistinguishable signal-to-noise ratio. We have also acquired spectra using the TPPI method [7,9,10]. The results (not shown) are essentially the same.

The equivalence of these spectra demonstrates the validity of the multiplex approach.

There is one experimental detail which must be closely attended to. Since the multiplex procedure involves phase shifts applied numerically in the computer after acquisition of the NMR signals, it is essential that the sense of these numerical phase shifts is the same as the that of the RF and digitizer phases applied by the spectrometer. As pointed out before [16,17], the sense of the RF and digitizer phase shifts depends in a complicated way on the sign of the gyromagnetic ratio of the resonant spins and on the radio-frequency mixing scheme employed in the spectrometer. The recommendations of Refs. [16,17] must be followed rigorously when implementing the multiplex procedure.

## 6. Conclusions

Together with cogwheel cycles [1], multiplex phase cycling opens up new possibilities for reducing the time span of some classes of NMR experiment. Examples include:

- The procedure sketched above may be applied directly to two-dimensional INADEQUATE spectroscopy in both liquids [18] and solids [15,19], leading to significant time savings in cases where the signal-to-noise ratio is good.
- The multiplex procedure applies to other forms of multiple-quantum spectroscopy. In general, the acquisition of pure-absorption  $(\pm p)$ -quantum spectra requires  $|4p|$  transients per  $t_1$  increment in the conventional SRH procedure, but only  $2|p| + 1$  transients per  $t_1$  increment in the multiplex procedure. The time saving approaches 50% for large  $p$ .
- Multiplex phase cycling may be used to obtain pure-absorption two-dimensional single-quantum spectra, with suppression of axial peaks, using 3 phase cycling steps instead of 4.
- In multiple-quantum magic-angle spinning experiments in solids [20–24], it should be possible to acquire signals simultaneously from many different

multiple-quantum pathways, obtaining complementary information without repetition of the experiment.

- In complex multidimensional experiments, particularly in solution NMR, there are prospects for combining the cogwheel or multiplex schemes with the limited use of field gradients, in order to combine the advantages of field gradients (for example, robust solvent peak suppression) with the superior signal strength of phase cycling.
- There are some pathway selection tasks which are problematic in the conventional method [4], but which are made possible by multiplexing. For example, consider a hypothetical experiment which requires selection of signal pathways involving the order changes  $\{0 \rightarrow \pm 1\}$ , while ensuring that the following order changes are suppressed:  $\{0 \rightarrow 0\}$ ,  $\{0 \rightarrow \pm 2\}$ ,  $\{0 \rightarrow \pm 3\}$ . Conventional two-step phase cycling can accomplish selection of  $\{0 \rightarrow \pm 1\}$  while suppressing  $\{0 \rightarrow 0\}$  and  $\{0 \rightarrow \pm 2\}$ , but cannot block the pathways  $\{0 \rightarrow \pm 3\}$  at the same time. Multiplex phase cycling allows the full completion of the selection task, using 5 acquired transients.

It is advantageous (but not necessary) to combine multiplex phase cycles with cogwheel phase cycles. In fact, the multiplex cycles described in this article are already simple examples of this. For example, the multiplex cycle described in Eqs. (10) and (11) may be notated [1] as COG5(1,0;0,0, $\pm 2$ ), where the winding numbers inside the parenthesis control the phase of the excitation block, the phase of the reconversion block, the receiver reference phase, the digitizer phase, and the two values of the numerical phase shift, respectively. The phase winding numbers of the radio-frequency pulses and the signal detection chain are separated by a semicolon. Similarly, the cycle in Eq. (18) and Eq. (19) may be notated COG5(0,1;0,0,2 $\pm 4$ ). Aside from their concrete advantages, the cogwheel and multiplex approaches provide a concise and unambiguous method for *notating* phase cycles.

At this moment, it is unclear as to whether multiplex and cogwheel phase cycles have any disadvantages, apart from increased data storage requirements. Since it is technically easier to generate accurate RF phase shifts in integer multiples of  $\pi/2$  than less usual subdivisions of  $2\pi$ , phase inaccuracy and instability may be an issue on some spectrometers, especially those that do not use direct digital synthesis (DDS) technology. However, we have seen no evidence of such problems, so far.

Data storage continues to become cheaper and computers continue to evolve in power. In future, it may become commonplace to store *all* acquired transients in the computer memory. This large data set would then be

processed in a multiplex fashion to retrieve signals from many different coherence transfer pathways.

## Acknowledgments

We thank Ole Johannessen for instrumental support and Andreas Brinkmann for discussions and help. C.E.H. has received support from the Marie Curie Fellowship Program (Grant HPMF-CT-1999-00199).

## References

- [1] M.H. Levitt, P.K. Madhu, C.E. Hughes, *J. Magn. Reson.* 155 (2002) 300–306.
- [2] J. Ollerenshaw, R.E.D. McClung, *J. Magn. Reson.* 143 (2000) 255–265.
- [3] D.J. States, R.A. Haberkorn, D.J. Ruben, *J. Magn. Reson.* 48 (1982) 286–292.
- [4] M.H. Levitt, *Spin Dynamics. Basics of Nuclear Magnetic Resonance*, Wiley, Chichester, UK, 2001.
- [5] A.D. Bain, *J. Magn. Reson.* 56 (1984) 418–427.
- [6] G. Bodenhausen, H. Kogler, R.R. Ernst, *J. Magn. Reson.* 58 (1984) 370–388.
- [7] R.R. Ernst, G. Bodenhausen, A. Wokaun, *Principles of Nuclear Magnetic Resonance in One and Two Dimensions*, Clarendon Press, Oxford, 1987.
- [8] Y.K. Lee, N.D. Kurur, M. Helmle, O.G. Johannessen, N.C. Nielsen, M.H. Levitt, *Chem. Phys. Lett.* 242 (1995) 304.
- [9] G. Drobny, A. Pines, S. Sinton, D.P. Weitekamp, D. Wemmer, *Faraday Div. Chem. Soc. Symp.* 13 (1979) 49.
- [10] D. Marion, K. Wüthrich, *Biochem. Biophys. Res. Commun.* 113 (1983) 967.
- [11] R. Freeman, S.P. Kempell, M.H. Levitt, *J. Magn. Reson.* 34 (1979) 663.
- [12] P. Bachmann, W.P. Aue, L. Müller, R.R. Ernst, *J. Magn. Reson.* 28 (1977) 29.
- [13] A. Hagemeyer, K. Schmidt-Rohr, H.W. Spiess, *Adv. Magn. Reson.* 13 (1989) 85.
- [14] G. Metz, X. Wu, S.O. Smith, *J. Magn. Reson. A* 110 (1994) 219.
- [15] A. Brinkmann, M. Edén, M.H. Levitt, *J. Chem. Phys.* 112 (2000) 8539–8554.
- [16] M.H. Levitt, *J. Magn. Reson.* 126 (1997) 164–182.
- [17] M.H. Levitt, O.G. Johannessen, *J. Magn. Reson.* 142 (2000) 190–194.
- [18] A. Bax, R. Freeman, T.A. Frenkiel, M.H. Levitt, *J. Magn. Reson.* 43 (1981) 478–483.
- [19] A. Lesage, M. Bardet, L. Emsley, *J. Am. Chem. Soc.* 121 (1999) 10987–10993.
- [20] L. Frydman, J.S. Harwood, *J. Am. Chem. Soc.* 117 (1995) 5367–5368.
- [21] G. Wu, D. Rovnyak, R.G. Griffin, *J. Am. Chem. Soc.* 118 (1996) 9326–9332.
- [22] A.P.M. Kentgens, R. Verhagen, *Chem. Phys. Lett.* 300 (1999) 435–443.
- [23] P.K. Madhu, A. Goldbourt, L. Frydman, S. Vega, *Chem. Phys. Lett.* 307 (1999) 41–47.
- [24] T. Vosegaard, P. Florian, P.J. Grandinetti, D. Massiot, *J. Magn. Reson.* 143 (2000) 217–222.